Continuous Tapered Fibers as Sensors for Cellular Growth and Pathogen Detection

Angela S.Y. Leung, Kishan Rijal, Gregory J. Thomas and Raj Mutharasan
Department of Chemical Engineering
Drexel University, Philadelphia, PA 19104

P. Mohana Shankar
Department of Electrical and Computer Engineering
Drexel University, Philadelphia, PA 19104

ABSTRACT

Tapered fiber biosensors were fabricated by heating and pulling single mode step-index fibers to waist diameters of 6-15 microns and lengths up to 2 mm. The effect of taper geometry on light transmission was explored theoretically and experimentally. Selected tapers were covalently bonded to antibodies to target molecules or cells. Sensing of antibody, bovine serum albumin (BSA), and the pathogen Escherichia coli O157:H7 was demonstrated for light source wavelengths of 470nm, 806nm, 550nm, and 1550nm.

KEYWORDS E. coli O157:H7 optical evanescent sensor

INTRODUCTION

In analytical, clinical, environmental, and pharmaceutical applications, efficient and accurate sensing of biomolecules and cells are highly beneficial [1-16]. To date, most measurements of cell concentration are done on large volumes. However, only small quantities of cells and tissues are available from biopsy or microbioreactors. As a result, it is necessary to develop biosensors which can quickly and accurately determine cell concentration with a small amount of sample.

Optical fibers are often used in spectroscopy because of their compatibility with the existing instrument. They are also used as sensors of chemicals, biomolecules, and physical properties such as strain.

Light is launched into a fiber in two components. The component inside the core of the fiber is considered guided, while the component outside the core is unguided and decays exponentially. This decaying field is called the evanescent field. Evanescent field is the component which interacts with samples. In normal fibers, evanescent field is small, so even though it interacts with samples, it stays outside the core and is not detected. By tapering, higher modes of light are supported, therefore more light will get into the evanescent domain and interact with the sample [17]. As the diameter increases again, some of that evanescent light can enter into the untapered region and be detected as output transmittance.

The fabrication of tapered fibers is achieved by heat pulling. The optical properties are determined by 1) the wavelength of the source, 2) the lengths of the contracting and expanding regions, and 3) the radius of the constant radius waist region.

In this paper we use tapered fibers to detect three analytes to demonstrate their potential as biomolecule or cell sensors.

MATERIALS AND METHODS

A silica, single mode (at 1300 nm), Corguide optical fiber (Corning Glass Works, NY, attenuation at 1300 and 1500 nm of 0.36 and 0.26 dB/m, respectively) with a core diameter of 8 um and total diameter of 125 um was used for all the experiments reported here. The polyacrylic sheathing was removed completely by a heated fiber stripper provided with the Ericsson FSU 975 fusion splicer .

Fiber Tapering

The fiber was then cleaned with isopropanol, and the ends were cut clean using a fiber cleaver provided with the FSU 975. Tapered region was incorporated into a fiber in two ways. In the first method, the fiber was inserted into the programmable FSU975 fusion

splicer and held together by clamps on both sides. Electric current was applied via a pair of electrodes for up to 60 seconds while the fiber is being pulled according to a preset program. Electric current levels and time can be altered in program parameters pre-defined by the splicer hardware. If an asymmetric taper was desired, one of the clamps was disengaged and used as a free weight attached to one end of the fiber. A picture of a typical taper is shown in Fig. 1

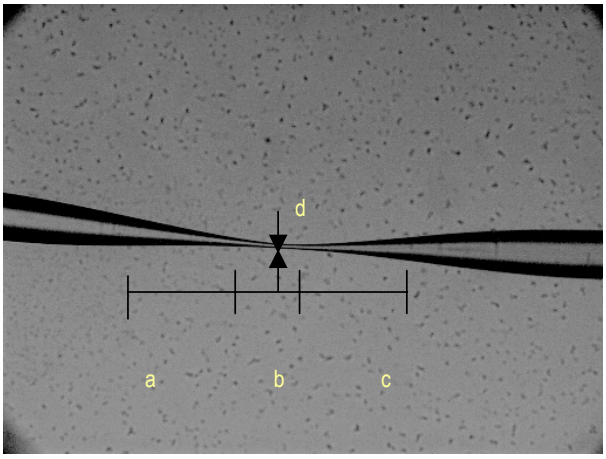

Figure 1: SEM micrograph of a typical taper.

The second method, heat pulling, was achieved by manually applying weight to both sides of the fiber while using a propane flame (described in [14]). Briefly, a bare fiber was mounted with two paper clips of identical weights (2.8 g) on either ends to provide tension. A micro flame (Model 6000, Microflame, Inc., MN) connected to propane and oxygen tanks was used to taper the fiber. After the formation of the taper, either ends of the fiber were cleaved using a fiber-optic cleaver (NO-NIK) to give orthogonal cut ends.

After tapered, the fiber was placed in an optical fiber holder (OFH) and used in the experiments. The OFH is described in our previous paper [14].

THEORETICAL CONSIDERATIONS

Stepwise Model for a tapered fiber

Consider the fiber's radius changes as a function of distance, z (see Figure 2). The fiber can support several modes of transmission specified by the V parameter of the fiber:

$$V_{core} = \frac{2\pi r}{\lambda}\sqrt{n_{core}^{\ 2} - n_{cl}^{\ 2}} \qquad (1)$$

Here, n_{core} is the refractive index of the core, n_{cl} is the refractive index of the cladding, and r is the radius of an untapered fiber [23].

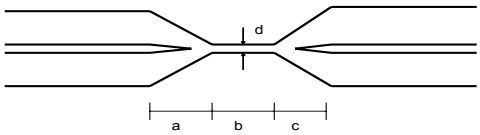

Figure 2: Geometry of a taper.

Assuming that light is launched axially, the only modes that will be supported will be the LP_{0m} modes [17]. When tapering starts, the coupling of modes takes place because of the perturbations introduced by the change in radius. As the diameter decreases, the core vanishes and the light guidance will be controlled by the cladding and the surrounding medium. It has also been shown that the start of the coupling of modes is defined by $V_{core}<1$. Beyond the location where V_{core} becomes less than 1, the light guidance is controlled by V_{clad}, as given by:

$$V_{clad}(z) = \frac{2\pi}{\lambda}\rho(z)\left[n_{cl}^{\ 2} - n_{ext}^{\ 2}\right]^{1/2} \qquad (2)$$

where n_{ext} is the refractive index of the surrounding medium and ρ is the radius at point z.

The light guidance in tapered fibers can be described using a stepwise model of the fiber as illustrated in Figure 3. We can write the amplitude of the modes at each step from the amplitudes of the modes of the previous step. This equation can be easily solved to obtain the output power.

$$V^{i} = \frac{2\pi}{\lambda}\rho^{i}\left[n_{cl}^{\ 2} - n_{ext}^{\ 2}\right]^{1/2} \qquad (3)$$

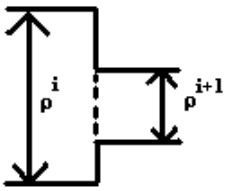

Figure 3: Picture of a step change in radius of the fiber.

In the case of no bending, the relationship between step i and step i+1 is:

$$\sum_{n=0}\sum_{m=1} a_{nm}^{i} E_{nm}^{i}(r) e^{-j\beta_{nm}^{i} z^{i}} = \sum_{p=0}\sum_{q=1} b_{pq}^{i+1} E_{pq}^{i+1}(r) e^{-j\beta_{pq}^{i+1} z^{i+1}} \quad (4)$$

Where E(r) is the electric field and β is the propagation constant. The coefficients b_{pq} were solved using the orthogonality of modes. A program was written in MATLAB to determine the coefficients in the model, and power is proportional to b_{pq}^{2}. In the program, parameters such as taper geometry, wavelength, and number of steps can be changed. The resulting power transmitted in the core at the output end is a function of all these factors.

Taper Characterization

The diameter and the total length of the tapered region were used to characterize the physical geometry of the tapered fibers. Pictures of the taper were taken via a video camera installed inside the FSU 975 splicer or an IMT-2 optical microscope (Olympus, Japan) was used in the case of a manually pulled taper. The length of the taper was measured using the Scion Image software (Scion Corp., MD) using a calibration. Typical taper geometry is shown on Figure 1.

Using an experimental setup similar to Figure 4, spectra were obtained for each tapered fiber in air and then with water in the tapered region. The light sources used included a LS-450 Blue LED (Ocean Optics), a 806nm laser diode, a 75W Xenon arc lamp (Ushio Inc., Japan) and a 1550nm laser diode (Thorlabs). Both pieces of equipment were coupled to the fiber via SMA or FC connectors. For the 470nm and 806nm sources, a CCD detector (USB2000, Ocean Optics) was used for measuring light transmission and the spectra were recorded onto a computer. For 1550nm light source, an optical spectrum analyzer (Ando AQ-6310B) was used to collect the data, and the data were transcribed manually into Excel. For the 550nm source, data was collected using a PMT (PTI Inc. P1572P) which was interfaced with a computer and FELIX software for data collection.

Antibody Immobilization

Silanol groups were produced on the surface of the tapered region by the following cleaning procedure: 1) taper was exposed to HCl:CH_4(1:1 by volume) solution at 25^{o}C for 30 min, then it was rinsed with deionized water. 2) Taper was exposed to H_2SO_4 at 25^{o}C for 30 min, then rinsed with deionized water. 3) It was immersed in 10M NaOH for 10 min at 80^{o}C, then rinsed with deionized water. 4) It was immersed in deionized water at 80 ^{o}C for 40 min.

Two approaches were used to silanize the taper with 3-aminopropyltriethoxysilane (APTES, Fluka, PA). In the first method, the taper was immersed in a 10% by volume APTES aqueous solution, pH 3-4, at 70^{o}C for 2 h. Then it was rinsed with deionized water and dried overnight at 75^{o}C. In the second method, the taper was immersed in a 2% by volume APTES acetone solution for 30 s, then rinsed with acetone. It was then dried for 10 min.

The carboxyl groups present in the monoclonal antibody to E. coli 0157:H7, IgG_2 (Kirkegaard and Perry Lab (KPL), Gaithersburg, MD) were activated by adding 0.5μL EDC (Fluka) and 1.1 mg of sulfo-NHS (Fluka) per ml of 0.1 mg/ml antibody solution in PBS for 30 min. Then, 0.5 μL of 2-mercaptoethanol (Sigma) was added to quench the EDC. The resulting solution containing antibody with activated carboxyl is allowed to react at room temperature for 2 h with the aminated taper surface**.**

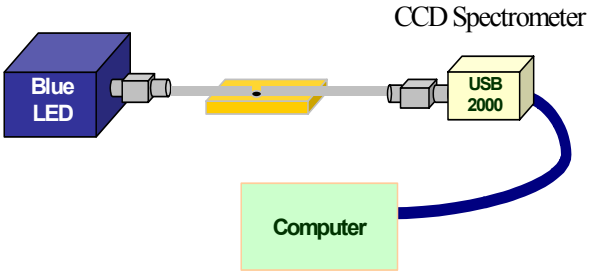

Figure 4: Typical setup of equipment for taper characterization or medium detection.

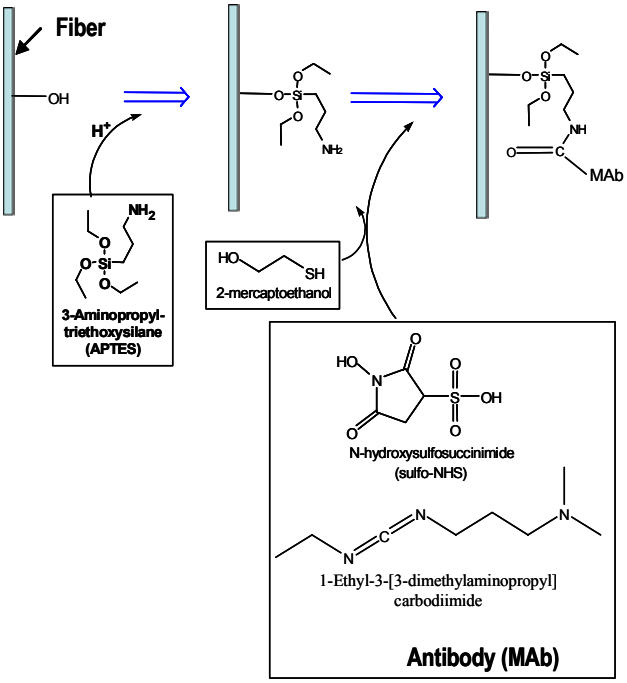

Figure 5: Reaction for antibody immobilization to fiber surface. Silanol reactive groups were produced on the glass surface by cleaning, then the surface was silanized by adding APTES. The coupling of the aminated surface and carboxyls on the antibody was mediated by zero-length crosslinking using sulfo-NHS and EDC. 2-mercaptoethanol was added quench excess EDC.

Cell Immobilization and Release

After the antibody was covalently linked to the fiber surface, the sensitized taper was submerged in a solution containing the corresponding antigen for 1 to 2 h. The captured antigen was released from the tapered surface by using a buffer pH 2 solution for 1h.

RESULTS AND DISCUSSION

Detection of E. coli O157:H7 and release

Attachment of antibody to E.coli O157:H7 was done with 470nm, 806nm, 550nm, and 1550nm light sources using different tapered fibers. In general, when the antibody solution was added, an immediate increase or decrease in transmitted light intensity first occurred due to change in refractive index of the surrounding liquid. Subsequently, there was a gradual and, often a smaller change in intensity occurred as the antibody reacted with the silanized glass surface and altered the optical characteristics of the evanescent field. The increase was observed in all nine experiments conducted. Out of these experiments, three were done at 806nm and 470nm, one was done at 550nm, and two were done at 1550nm. The experiments performed using the 470nm were repeated experiments with the same fiber re-cleaned and re-attached, as with the experiments at 1550nm. The most pronounced change was observed in one of the 470nm experiments (see Fig. 6).

For E. coli detection, intensity gradually decreased in eight out of total nine experiments conducted. In the case when there was an increase, the increase was less than 5%. The largest decrease of intensity was -40% and occurred with the 550nm light source.

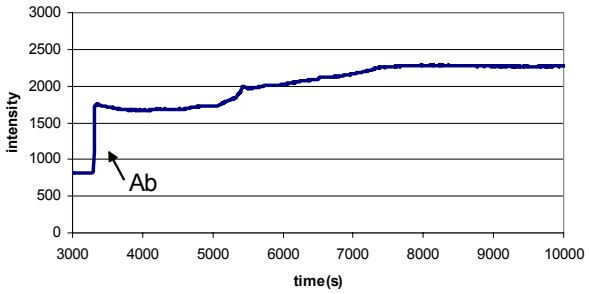

Figure 6: Transmission vs. time for antibody attachment using a 470nm LED light source. Dimensions are a=123.5µm, b=126.8µm, c=455.9µm , d=6.3µm.

For the results shown in Figures in 7a and 7b, a manually heat-pulled tapered fiber was used. The taper was silanized and immobilized with antibody as described earlier. After soaking the taper in PBS (pH 7.4) for 2 h, E. coli O157:H7 (KPL, Laboratories Inc.,

MD, concentration $7x10^7$ cells/ml) was injected into the sample chamber in the fiber holder. After attachment the E. coli solution was pipetted out and 0.1M glycine HCl in 50% (v/v) ethylene glycol buffer (pH 1.7) was added to release the antigens attached to the antibody on the fiber. As seen in Figure 7a, there was a 7% decrease in transmission during E. coli O157:H7 attachment and approximately the same percentage increase in transmission during release (Figure 7b).

Transmission through the fiber decreased during attachment of E. coli 0157:H7 cells to antibody immobilized taper. This occurs as the attached cells absorb light launched from the convergent side of the taper and thus reduce transmission. During release, cells are detached from the taper, thus minimizing interaction between the cells and evanescent field, resulting in an increase in transmission.

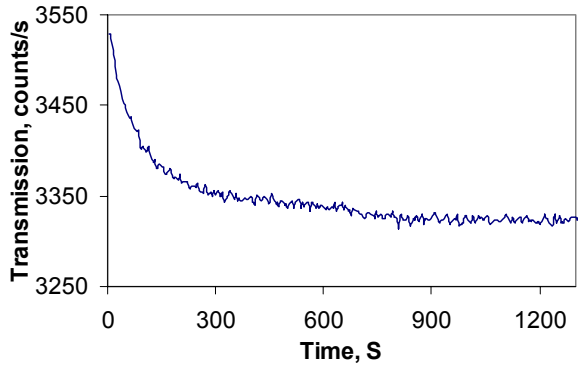

Figure 7a

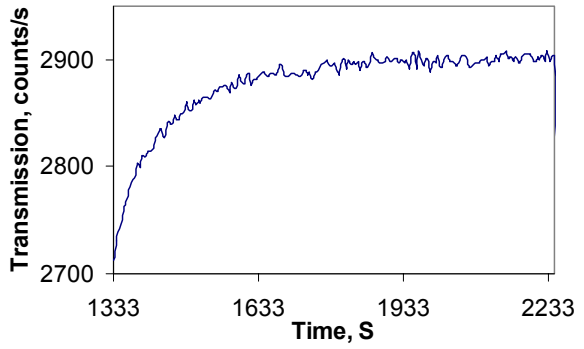

Figure 7b

Figure 7: Continuous E. coli O157:H7 attachment & release with a flame drawn fiber. a) Drop in Transmission of light during attachment b) Increase in transmission of light through the fiber when the taper is immersed in 0.1M glycine HCl in 50% (v/v) ethylene glycol buffer (pH 1.7). Approximate taper dimensions are a=125 µm, c=560 µm, b=80 µm, d=9.5 µm.

BSA Binding

Several anti-BSA immobilizations were carried out using 470nm and 806nm light sources over different lengths and diameters of asymmetrical tapered fibers. A total of five experiments involving these asymmetrical fibers were done. Two of the five experiments performed were done using the 470nm LED; the other three were performed using the 806nm laser. A sharp, immediate increase or decrease was observed with the addition of the antibody solution, 0.1mg/mL anti-BSA in PBS pH 7.4.

Significant attachment of BSA was not observed in any of the five experiments when the tapered fiber was submerged in a 1mg/mL BSA in PBS pH 7.4. Minimal amounts of increased intensity occurred, and this change may be attributed to small source fluctuations.

In four of the five experiments conducted, minimal changes in intensity could be observed (< 5%) when the tapered fiber was immersed in the release buffer pH 2.2. However, a gradual and large increase in intensity was observed in one of them. The intensity change increased a total of one thousand counts during the 1 hour in which the tapered fiber was immersed in the HCl buffer. This change was observed using the 806 nm light source (See Figure 8).

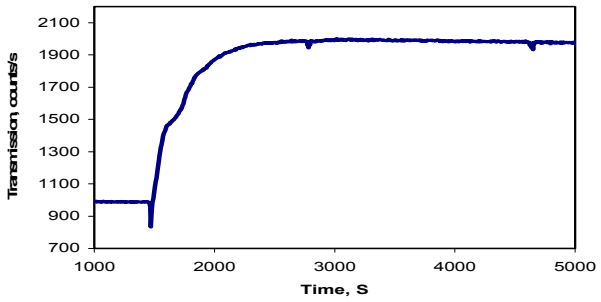

Figure 8: Intensity vs. Time for a tapered fiber. Taper dimensions are a=196.2µm, b=501.7µm, c=438.3µm, d=12.8µm

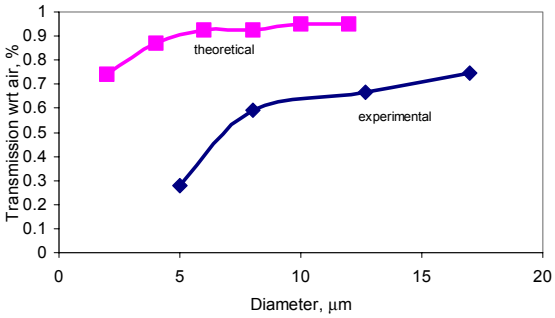

Figure 9: Transmission in water vs. diameter for a short taper. Dimensions are a=50µm, b=25µm, c=50µm.

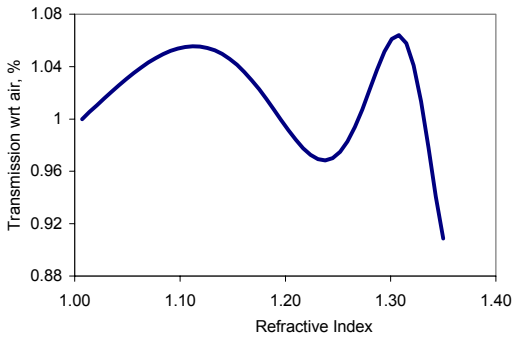

Figure 10: MATLAB simulation for Exp III, dimensions are a=312µm, b=1000µm, c=105 µm, d=8µm.

Effect Taper Geometry on Transmission

Using the calculation procedure previously described, theoretical transmission was obtained by keeping the length of symmetric tapers constant while varying the diameter. Experimental results appear to have similar trends as the simulation. Fig 9 shows this result for a short taper. Medium and long tapers exhibit similar behavior. All of the symmetric tapers had lower transmission in water compared to in air.

On the other hand, asymmetric tapers showed a higher transmission in water compared to air depending on the geometry. Table 1 summarizes experiments carried out in 1550nm and 470nm for two asymmetric tapers, and Fig 10 is a MATLAB simulation for taper 2. The simulation shows that for an asymmetric taper, the normalized transmission in water may be higher than one. This agrees well with the experimental results qualitatively. From the foregoing, it is clear that transmission through a taper due to a change in refractive index in the medium is quite complex and is dependent on the taper geometry.

Table 1: Percentage change of transmission in water compared to in air for 2 tapers in 1550nm and 470nm source sources. Dimensions are taper 1: a=123.7µm, b=223.2µm, c=549.1µm, d=12.7µm; taper 2: a=145.6µm, b=1097.4µm, c=571.2µm, d=6.33µm.

	Taper 1	Taper 2
1550nm	0.69±0.02	1.4±0.3
470nm	0.69±0.09	

In the current context, the taper that exhibits the largest change in evanescent field following a change in the refractive index of the liquid in its immediate vicinity is likely to provide good sensitivity. Based on the study done to date it is reasonable to conclude that asymmetric tapers exhibits higher sensitivity, and longer tapers are more suitable for sensing.

SUMMARY

In this paper we have shown that: (1) Antibody binding to the taper can be detected optically (2) E. coli attachment to the taper can be detected (3) BSA release can be detected. (4) The radius, expanding length and contracting length have significant effects on transmission characteristics.

ACKNOWLEDGMENTS

This research was supported in part by funding from the State of Pennsylvania under The Nanotechnology Institute and the National Science Foundation grant BES 0329793.

REFERENCES

1. J. Keirss, C. Boussard-Pledel, O. Loreal, O. Sire, B. Bureau, P. Leroyer, B. Turlin, J. Lucas, *IR*

optical fiber sensor for biomedical applications, Vibrational Spectroscopy, 2003, 32: p. 23-32.
2. P. Ferreira, M.M. Werneck, and R.M. Ribeiro, *Development of an evanescent-field fibre optic sensor for Escherichia Coli O157:H7*. Biosensors and Bioelectronics, 2001. **16**: p. 399-408.
3. M.I. Daneshvar, J.M. Peralta, G.A. Cassay, N. Narayanan, Lawrence Evans III, G. Patonay, L. Strekowski, *Detection of biomolecules in the near-infrared spectral region via a fiber-optic immunosensor*, Journal of Immunological Methods, 1999, 226: p.119-128.
4. Brian M. Cullum, Guy D. Griffin, Gordon H. Miller, and Tuan Vo-Dinh, *Intracellular Measurements in Mammary Carcinoma Cells using fiber-optic nanosensors*, Analytical Biochemistry, 2000, 227: p.25-32.
5. U. Bindig, M. Meinke, I. Gersonde, S. Kravchik, S. Citron, A. Katzir, G. Muller, *Detection of malignant tissue by using infrared microscopy and fiberoptic spectroscopy.* Proceedings of SPIE, 2001. 4253 (Optical Fibers and Sensors for Medical Applications): p. 108-117.
6. J.-W. Choi, J.H. Park, S.C. Lee, D.-I. Kim, W.H. Lee, *Analysis of culture flouorescence by a fiber-optic sensor in Nicotiana Tabacum plant cell culture.* Korean Journal of Chemical Engineering, 1995. **12**(5): p. 528-534.
7. Chuang, H., P. Macuch, and M.B. Tabacco, Optical sensors for detection of bacteria. 1. General concepts and initial development. Analytical Chemistry, 2001. **73**: p. 462-466.
8. B.M. Cullum, G.D. Griffin, G.H. Miller, T. Vo-Dinh, *Intracellular measurements in mammary carcinoma cells using fiber-optic nanosensors.* Analytical Biochemistry, 2000. **277**: p. 25-32.
9. S. McCulloch and D. Uttamchandani, *Development of fibre optic micro-optrode for intracellular pH measurements.* IEE Proceedings-Optoelectronics, 1997. **144**(3): p. 162-167.
10. S. Pilevar, C.C. Davis and F. Portugal, Tapered optical fiber sensor using near-infrared fluorophores to assay hybridization. Analytical Chemistry, 1998. **70**(10): p. 2031-2037.
11. N. Nath, S.R. Jain and S. Anand, Evenescent wave fibre optic sensor for detection of L. donovani specific antibodies in sera of kala azar patients. Biosensors and Bioelectronics, 1997. **12**(6): p. 491-498.
12. T. Vo-Dinh, J.-P. Alarie, B.M. Cullum, G.D. Griffin, *Antibody-based nanoprobe for measurement of a fluorescent analyte in a single cell.* Nature Biotechnology, 2000. **18**: p. 764-767
13. C. Zhou, P. Pivarnik, S. Auger, A. Rand, S. Letcher*, A compact fiber-optic immunosensor for Salmonella based on evanescent wave excitation.* Sensors and Actuators B, 1997. **42**: p. 169-175.
14. H. Haddock, P.M. Shankdar, R. Mutharasan, *Evanescent sensing of biomolecules and cells.* Sensors and Actuators B, 2003. **88**: p. 67-74.
15. P. Wiejata, P.M. Shankar, R. Mutharasan, *Fluorescent sensing using biconical tapers*. Sensors and Actuators B, in press, 2003.
16. C. Bariain, I.R. Matias, F.J. Arregui, M. Lopez-Amo*, Tapered optical-fiber-based pressure sensor.* Optical Engineering, 2000. **39**(8): p. 2241-2247.
17. Lloyd C. Bobb, P.M. Shankar, Howard D. Krumboltz, Bending effects in biconically tapered single-mode fibers, *Journal of Lightwave Technology*, 1990, 8(7): p.1084-1090.
18. L.C. Shriver-Lake, B. Donner, R. Edelstein, K. Breslin, S.K. Bhatia, F.S. Ligler, *Antibody immobilization using heterobifunctional crosslinkers*. Biosensors and Bioelectronics, 1997. **12**(11): p. 1101-1106
19. Q. Weiping, X. Bin, Y. Danfeng, L. Yihua, W. Lei, W. Chunxiao, Y. Fang, L. Zhuhong and W.Yu, *Site-directed immobilization of immunoglobulin G on 3-aminopropyltriethoxylsilane modified silicon wafer surfaces*. Materials Science and Engineering C, 1999. 8-9: p. 475-480.
20. H. Shirahama, and T. Suzawa, *Adsorption of Bovine Serum Albumin onto styrene/acrylic acid copolymer latex*, Colloid and Polymer. Science, 1985. 263: p. 141.
21. R.M.C. Dawson, D.C. Elliott, W.H. Elliott, and K.M. Jones,,''*Data for Biochemical Research*,'' 3rd edition Oxford University Press, Oxford, 1986.
22. J.-Y. Yoon, H.-Y. Park, J.-H. Kim AND W.-S. Kim, *Adsorption of BSA on Highly Carboxylated Microspheres—Quantitative Effects of Surface Functional Groups and Interaction Forces*. Journal of Colloid and Interface Science, 1996. 177: p. 613-620.
23. John A. Buck, Fundamentals of Optical Fibers, John Wiley & Sons, Inc., USA, 1995.
24. Gerd Keiser, Optical Fiber Communications, McGraw-Hill Book Company, USA, 1983.

CONTACT

Mutharasan@drexel.edu